

Strategy for High Concentration Nanodispersion of Single-Walled Carbon Nanotubes with Diameter Selectivity

Chandan Biswas, Ki Kang Kim, Hong-Zhang Geng, Hyeon Ki Park, Seong Chu Lim,
Seung Jin Chae, Soo Min Kim, and Young Hee Lee*

Department of Physics, Department of Energy Science, Sungkyunkwan Advanced Institute of Nanotechnology, Center for Nanotubes and Nanostructured Composites, Sungkyunkwan University, Suwon 440-746, Republic of Korea

Michael Nayhouse and Minhee Yun*

Department of Electrical and Computer Engineering, University of Pittsburgh, Pittsburgh, Pennsylvania 15260

Received: February 25, 2009; Revised Manuscript Received: March 25, 2009

Nanodispersion of single-walled carbon nanotubes (SWCNTs) have been systematically investigated with the use of sodium dodecyl sulfate (SDS) and poly(vinylpyrrolidone) (PVP) surfactant in deionized water. A high concentration of nanodispersed SWCNTs up to 0.08 mg/mL was achieved with introduction of an additional dispersant of PVP by optimizing surfactant concentration, sonication time, and centrifugation speed, which was crucial to obtaining a high concentration of SWCNTs in the supernatant solution. We also demonstrate that diameters of the nanodispersed nanotubes can be sorted out by controlling the centrifugation speed, and furthermore, the saturated SWCNT concentration was nearly constant, independent of the initial concentration at high centrifugation speed. Two dispersion states were identified depending on the centrifugation speed: (I) an intermediate mixed state of nanodispersion and macrodispersion and (II) nanodispersion state. This was verified by Raman spectroscopy, scanning probe microscopy, optical absorption spectroscopy, and photoluminescence measurements. The obtained SWCNT solution was stable up to about 10 days. Some aggregated SWCNT solution after a long period of time was fully recovered to initial state of dispersion after resonication for a few minutes. Our systematic study on high concentration nanodispersion of SWCNTs with selective diameters provides an opportunity to extend the application areas of high quality SWCNTs in large quantity.

1. Introduction

Since the discovery of carbon nanotubes (CNTs) in the last decades of the 20th Century,¹ researchers have uncovered various potential characteristics which could be applicable to future device applications.^{2–11} Carbon nanotubes have superb mechanical strength, chemical stability, and high electrical conductivity,^{2,3} which constantly attracts the attention of researchers and engineers around the world in areas such as electronic devices,^{4,5} composite materials,^{6,7} and biosensors.⁸ However, for better and more specific device applications, customized nanotubes are required to improve performance. For example, the typical lengths of CNTs are in the order of nanometer to centimeter⁹ and exist in nature in the form of bundles. These bundled CNTs need to be individually separated to achieve better device performances in numerous applications.^{10–12} Due to their strong pi–pi interaction at the nanotube surface, the tube–tube interaction energy of micrometer-long CNTs is around 1000 eV.¹³ Due to this strongly shared attractive force, it is difficult to achieve a well-dispersed CNT solution by using physical approaches such as sonication, ball milling, or some chemical treatments. A precise combination of physical and chemical approaches such as sonication and surface functionalization is required to achieve good individual CNT dispersion.

The state of CNT dispersion in solvent can be classified in the following way: (i) macrodispersion, where several dozen of CNTs form a bundle but remain dissolved in solvent, and

(ii) nanodispersion, where individual CNTs are separated from each other and well dissolved in solvent.¹⁴ In the case of electronic devices, the controllability and optimization of the dispersion state plays a crucial role in improving the device performance. In addition to the dispersion state, there are other parameters that determine the performance of electronic devices. For instance, control of CNT concentration, and possibly chirality and diameter of the dispersed CNTs in the solution. Improvement of CNT dispersion can be accomplished by functionalizing the nanotube surface with various functional groups such as hydroxyl, amine, and carboxyl groups, or fluorinating the hydrophobic CNT surface into a hydrophilic surface.^{15,16} So far, there has been significant progress toward the solubility of single-walled carbon nanotubes (SWCNTs) in both organic and aqueous media. Organic solvents such as toluene, 1,2-dichloroethane, *N,N*-dimethylformamide (DMF), and *N*-methyl-2-pyrrolidone (NMP), have been examined without additives.^{14,17,18} Although an organic solvent approach is required for some applications, these are toxic and involve special care. Therefore, water-based dispersion of CNTs is often desirable for environmental purpose as well as in biomedical and biophysical processing. In order to disperse hydrophobic CNTs in a polar solvent like water, the CNT surface is typically covered by a surfactant such as sodium dodecyl sulfate (SDS), sodium dodecylbenzene sulfonate (NaDDBS),^{19–22,33} DNA,^{8,23} or various polymers.^{24–26,36,37} Although these approaches achieve some degree of nanodispersion of SWCNTs, the concentration of CNTs in solvent is extremely low in most cases (sometimes,

* Corresponding author. E-mail: leeyoung@skku.edu.

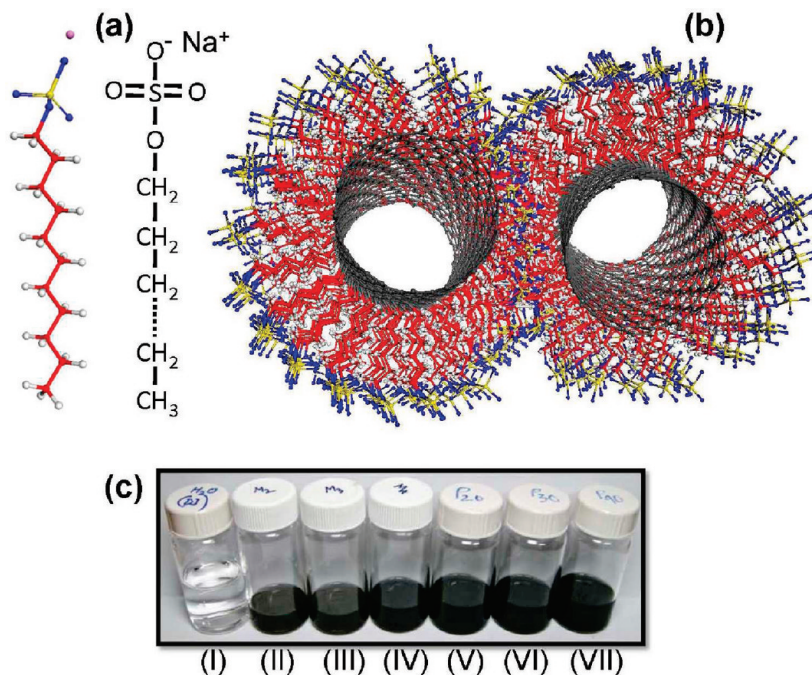


Figure 1. (a) Schematic (ball and stick model) of individual SDS molecule and its corresponding chemical structure, (b) Schematic of SWCNT surface functionalized by SDS molecules, which separates SWCNTs from its bundle and also dispersing into water, and (c) Optical micrograph of dispersed SWCNT solution with various surfactants; DI water (I), SWCNTs dispersed in water and sonicated for 20 min with SDS (II), and with SDS + PVP (V), SWCNTs dispersed in water and sonicated for 30 min with SDS (III) and with SDS + PVP (VI), SWCNTs dispersed in water and sonicated for 40 min with SDS (IV) and with SDS+PVP (VII). All the samples with 3 wt % SDS and 1 wt % PVP were sonicated at a sonication power density of 9.38 W/mL and centrifuged at 170 000g for 4 h after sonication.

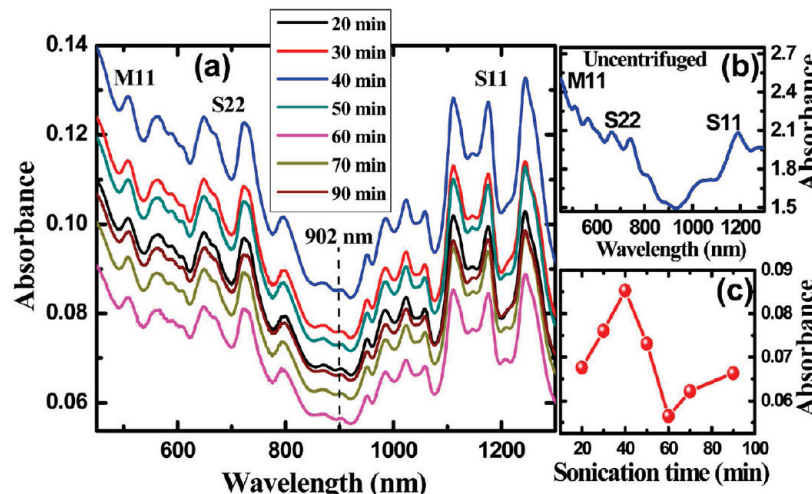


Figure 2. (a) Absorption spectra of SWCNTs (25 mg) dispersed in water (50 mL) with SDS (3 wt %) surfactant at a sonication power density of 9.38 W/mL and centrifuged at a speed of 170 000g for 4 h at different sonication times. (b) Normalized absorption of the sample same as (a) at a sonication time of 40 min but without centrifugation. (c) Absorbance value dependence on sonication time of all the samples of (a) at 902 nm wavelength of the absorption spectra.

not even visible with bare eyes). Highly concentrated nanodispersed CNT solution is necessary for various applications.³⁸ In addition, the control of diameter and chirality is required, if possible. Another important issue is the stability of the nano-dispersed CNT solution to be utilized for further use of applications.

The purpose of our work is 3-fold: (i) to achieve a high concentration nanodispersion of SWCNTs in water, (ii) to find rigorous methods of measurements to identify the degree of dispersion state including the stability of dispersion, and (iii) to accomplish diameter selective nanodispersion of SWCNTs and saturated SWCNT concentration in the solution by the

centrifugation method. In this study, SWCNTs have been dispersed in water by introducing PVP in addition to SDS to achieve high-concentration nanodispersion. The degree of dispersion was systematically controlled by optimizing the surfactant concentration, sonication time, and centrifugation speed. The dispersion state and the stability of the CNT solution were characterized by Raman spectroscopy, optical absorption spectroscopy, and photoluminescence. In this paper, we describe a method for calculating the concentration of SWCNTs after dispersion and centrifuge. The sorting of diameters of nanotubes was precisely controlled by changing the centrifugation speed.

2. Experimental Section

2.1. Optimization of Dispersion State of SWCNT. Our foremost aim was to optimize nanodispersion conditions of SWCNTs in water with surfactant. The unpurified SWCNTs synthesized by a high-pressure carbon monoxide (HiPCO) process were purchased from Carbon Nanotech Inc. Before adding SWCNTs, SDS (MW 288.38, purchased from Fluka Chemie GmbH) was dissolved in water homogenously and then 25 mg of SWCNT powder was dispersed in 50 mL of water with different SDS concentrations from 1 to 5 wt % to optimize nanodispersion. This SWCNT solution in a conical flask was sonicated for different times from 2 to 90 min. Homogenizer (ULSSO Hi-Tech, ULH 700S) was used for sonication with a sonication power density of 9.38 W/mL. A conical-shaped flask was taken as a sonication sample container to reduce the bubble formation during sonication, which induces bundling of CNTs. Immediately after sonication, the sample was centrifuged (LE-80K, Beckman Coulter) with a high speed of 170 000g, and only the supernatant of the produced solution was carefully decanted immediately after the centrifugation, leaving the bundled CNTs in the precipitated solution. The supernatant contained homogeneously nanodispersed SWCNT solution. To increase the nanodispersed SWCNT concentration by warping the SDS covered SWCNT with long PVP chain in the colloidal suspensions, PVP ($M_w = 55\ 000$) of 1 wt % was added before sonication, followed by a similar procedure as previously mentioned.

2.2. Sample Preparation for Dependence of CNT Concentration and CNT Diameter on Centrifugation Speed. For optimization of nanodispersed SWCNT concentration after centrifugation, the different amounts (from 0.008 to 0.06 wt %) of SWCNTs were added to the SDS-PVP-water (3 wt % SDS, 1 wt % PVP in 50 mL of water). This SWCNT solution was sonicated for 40 min at a sonication power density of 9.38 W/mL similar to the previous case. During sonication, the temperature of the solution was kept constant at 9 °C. The samples were centrifuged immediately after sonication for different centrifugation speeds starting from 15 000g to 376 300g for 4 h. The supernatant of the centrifuged solution was carefully taken and characterized by the following procedures.

2.3. Measurements. UV-vis-NIR absorption spectroscopy was performed using a Cary 5000 spectrophotometer (Varian, CA, USA). A quartz cell with a path length of 1 mm was used for these absorption measurements. The energy spectral range from 0.8 to 3 eV was scanned to obtain absorbance. The Raman system (Renishaw RM1000-Invia) was used to measure Raman shift of the dispersed SWCNTs through a laser excitation of 633 nm wavelength (excitation energy 1.96 eV) with a notch filter with 50 cm⁻¹ cutoff frequency to ensure the low energy radial breathing mode (RBM). Scanning probe microscope (SPM: Seiko SPA 400) with dynamic force microscopy (DFM) mode was used to measure the morphology of the deposited CNTs on Si substrate. The sample was further analyzed using a fluorescence analyzer (NS1 NanoSpectralyzer, Applied NanoF-fluorescence) with laser excitation energies of 1.94 (640 nm), 1.81 (683 nm), and 1.58 eV (786 nm) to verify the dispersion state, dispersion stability, and diameter dependence. In this case, a quartz cell with a 1 cm path length was used as a solution container.

3. Results and Discussion

3.1. Optimization of SWCNT Nanodispersion State. Figure 1a shows a schematic (ball and stick model) of an individual SDS molecule and its corresponding chemical formula. The tail

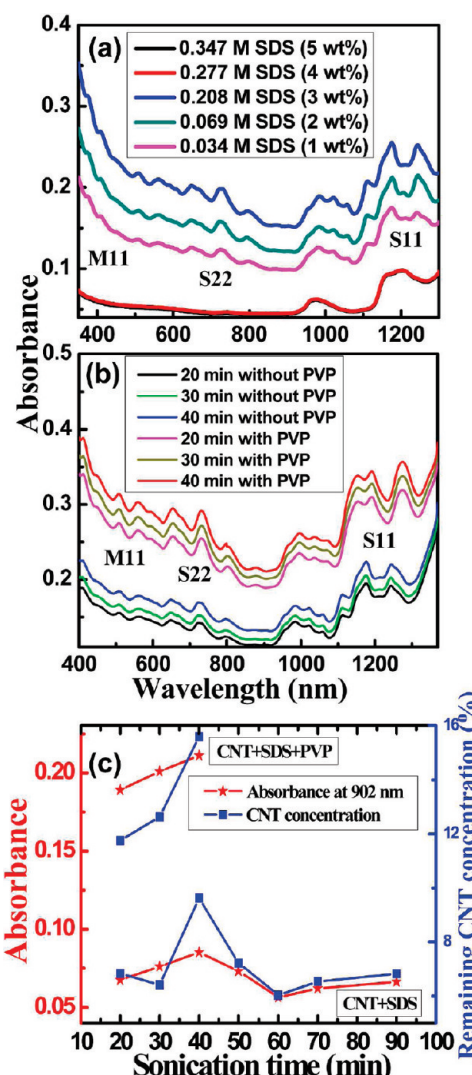


Figure 3. (a) Absorption spectra of SWCNTs (0.05 wt %) dispersed in water (50 mL) for different SDS concentrations at a sonication power density of 9.38 W/mL for 40 min sonication and followed by centrifugation for 4 h at 170 000g. (b) Absorption spectra of the CNT solution. All other conditions are the same as (a) but with PVP (1 wt %) and different sonication time. Here, SDS concentration was fixed at 3 wt %. (c) Absorbance at 902 nm and the remaining CNT concentration as a function of sonication time at different combination of surfactants.

group containing a hydrophobic alkyl chain wraps up to interact with the CNT surface and squeezes into the bundle of CNTs by sonication.²⁷ The headgroup containing the hydrophilic sulfonic group dissolves in water to enhance dispersion of separated CNTs. Due to the presence of the ionic headgroup of the surfactant, the whole CNT structure covered with surfactants can be dissolved in water. Figure 1b shows a schematic of an individual SWCNT covered by SDS molecules. Figure 1c shows an optical micrograph of SWCNTs dispersed in water with various conditions. From the photographs we observed that samples (V), (VI), and (VII) are darker than samples (II), (III), and (IV) due to the presence of higher SWCNT concentration in the solution. This was attributed to the use of additional PVP to enhance dispersion of SWCNTs. Although the difference between them is hardly distinguishable by the naked eye, it has been clearly verified by absorption spectroscopy as described later in the report (Figure 3b,c).

Figure 2 presents the absorption spectra of nanodispersed SWCNT solution. The absorption band is mainly composed of

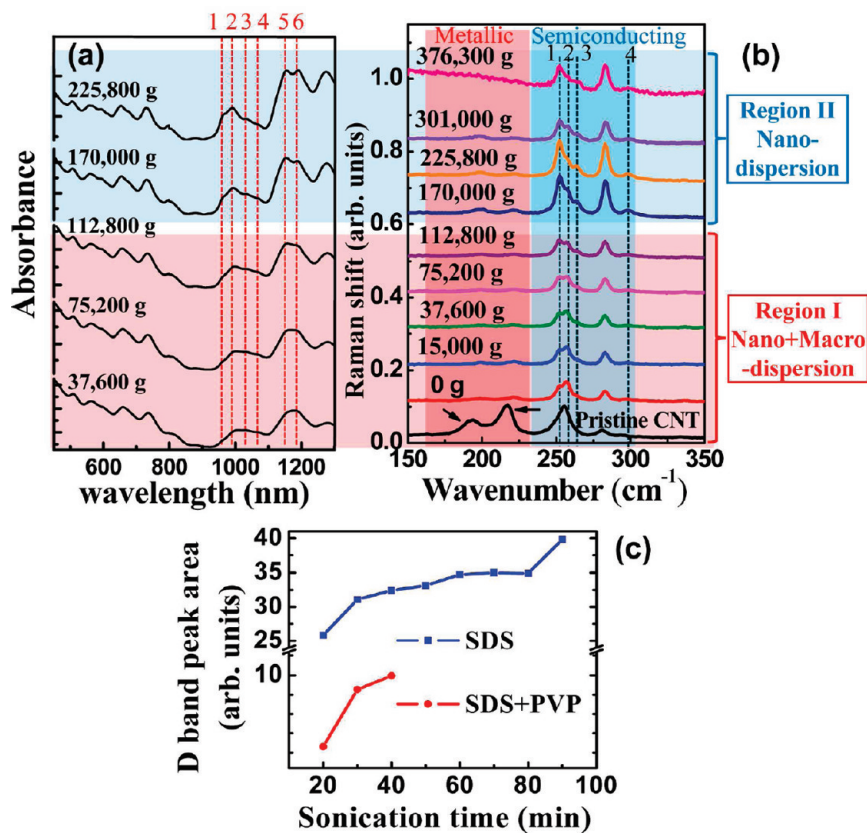


Figure 4. (a) Absorbance in terms of centrifugation speed from the SWCNT solution (0.06 wt % CNT, 3 wt % SDS, 50 mL water, 40 min sonication time, 9.38 W/mL power density, and 4 h centrifugation time). The dotted lines indicate the positions of subband peaks. (b) Raman spectra (RBM mode) in terms of centrifugation speed with a laser excitation energy of 1.96 eV (633 nm wavelength) from the same samples as (a). All the peaks are normalized by the G-band intensity at 1589 cm^{-1} wavenumber. The red and blue area in the Figure indicates the metallic and semiconducting nanotube region, respectively. (c) D-band peak area (obtained from Raman spectroscopy at 633 nm wavelength) dependent on the sonication time of CNT dispersed in SDS and SDS + PVP, respectively.

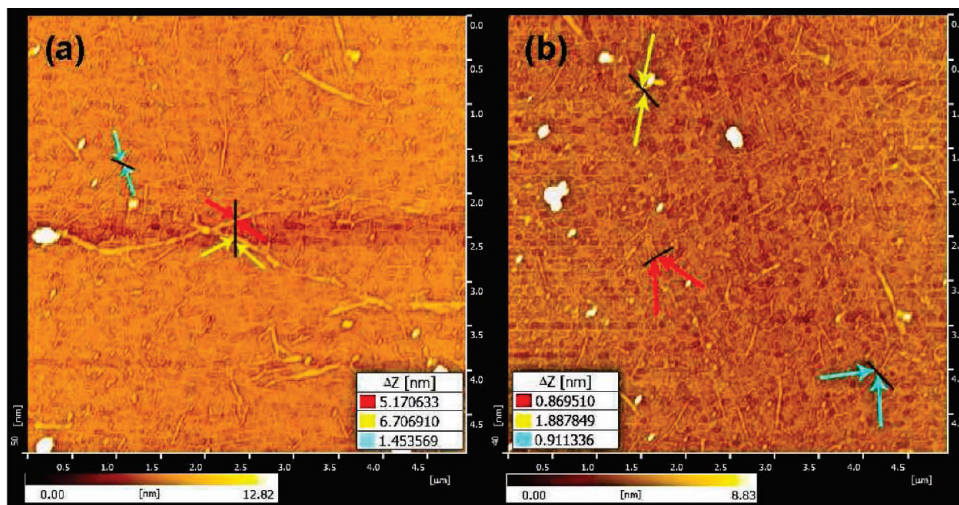


Figure 5. Scanning probe microscope (DFM mode) images of the SWCNTs deposited on silicon substrate. The SWCNT solution (0.06 wt % CNT, 3 wt % SDS, 50 mL water, 40 min sonication time, 9.38 W/mL power density) centrifuged for 4 h at a different centrifugation speed of (a) 112,800g (region I) and (b) 170,000g (region II) was deposited on a functionalized silicon wafer having 300 nm SiO_2 layer. Before taking these images the sample was washed by methanol for 3 min followed by 7 h heat treatment at 240°C in air to remove SDS on SWCNTs.

three regions: (i) the first allowed van Hove singularity transitions of semiconducting SWCNTs (E_{11}^S or S11); (ii) the second van Hove singularity transitions of semiconducting SWCNTs (E_{22}^S or S22), and (iii) the first van Hove singularity transitions of metallic ones (E_{11}^M or M11). Since the samples may have CNTs with different diameters and chiralities, many such corresponding subband peaks should exist even within the same S11, S22, and M11 bands. These are usually quenched

particularly in the case of S11, as can be seen in Figure 2(b), if the nanotubes remain bundled in the solution before centrifugation. After centrifugation, all the bands were split into numerous subbands, indicating a nanodispersion state, independent of the sonication time. Nevertheless, the absolute absorbance shows the maximum at a sonication time of 40 min, as shown in Figure 2(c). Since absorbance A is proportional to the CNT concentration, we have $A = \varepsilon \rho L$, where ε , ρ , and L are the extinction

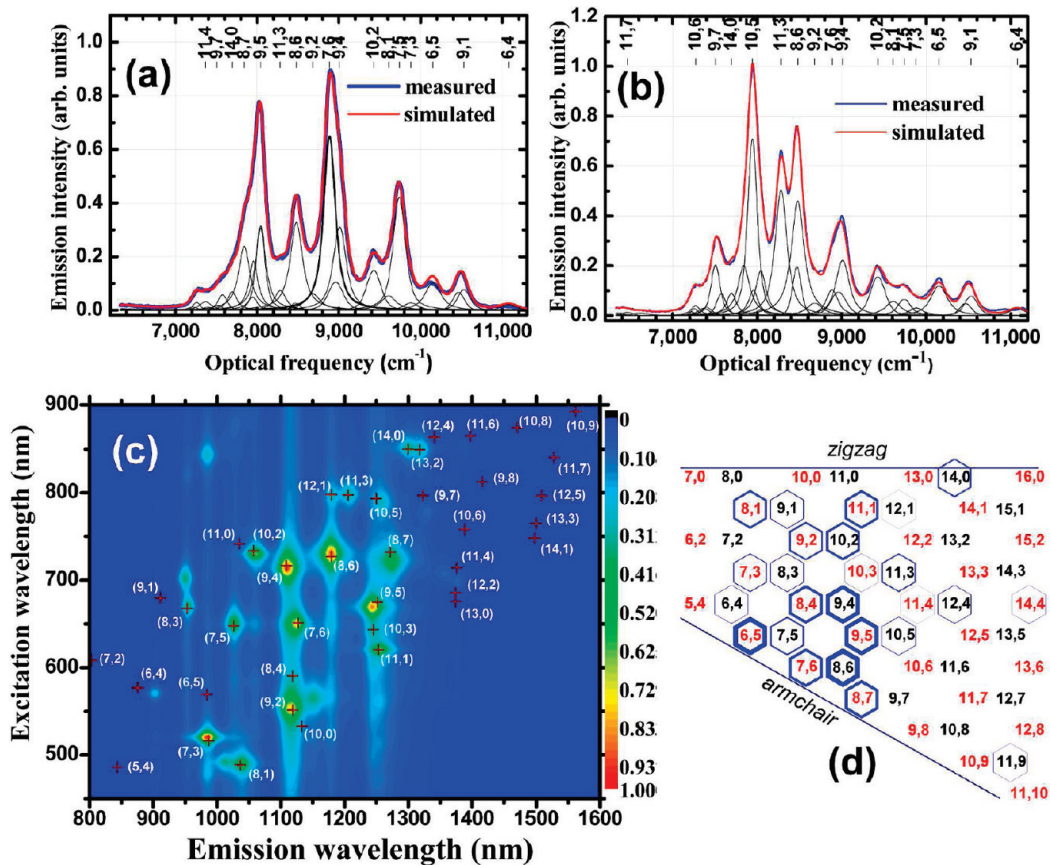


Figure 6. Measured and fitted (by Lorentzian shape) fluorescence for SDS-dispersed SWCNTs in water (0.05 wt % SWCNTs, 3 wt % SDS, 50 mL water, 40 min sonication time, 9.38 W/mL power density, and 170 000g centrifugation speed for 4 h) with a laser excitation energy of (a) 640 nm and (b) 783 nm. The corresponding calculated (n,m) indices are positioned on the top of the graph. (c) Contour plot of fluorescence intensity for excitation energy (1.94, 1.81, and 1.58 eV) vs emission wavelengths. The color indicates the strength of the emission. The marked points of indices are the theoretically calculated (n,m) indexes from semiempirical model^{31,32} and fitted with the experimentally obtained contours. (d) The corresponding (n,m) indices are plotted on a graphene sheet according to their strength from (c). The observed nanotube structures marked as blue hexagons, red and black (n,m) labels represent type 1: ($n-m$) mod 3 = 1 and type 2: ($n-m$) mod 3 = 2 graphene lattice points, respectively.

coefficient, concentration of SWCNTs in the medium, and path length, respectively; this ensures that the nanodispersed SWCNT concentration in the solution is the highest at 40 min among time durations. In this case, the absorbance was taken at a nonresonant region near 902 nm to get the density dependence of SWCNTs in the solution.

The SDS concentration was optimized at a SWCNT concentration of 0.05 wt % dispersed in water, as shown in Figure 3a. The absorbance increased initially at low SDS concentration and decreased abruptly beyond 3 wt %. The SDS concentration of 3 wt % (SDS:CNT = 3:0.05) has the highest absorbance. This value is relatively high compared to previous reports.^{28,33,34} At this condition, not only the SWCNTs were nanodispersed with distinct subbands, but also the CNT concentration was the highest. This condition has been proven in Figure 2. At high SDS concentrations of 4 and 5 wt %, SWCNTs were not nanodispersed, and the bundled SWCNTs are precipitated during centrifugation. As a consequence, low CNT concentration in the supernatant was obtained. The possible explanation might be related to the limit of surfactant coverage on the CNT walls. After the SDS concentration exceeds that limit, the surfactant entropic interactions induced by free surfactant micelles result in surfactant aggregation on the CNT walls, reducing the dispersion of the CNT bundles in water.³⁵

Figure 3b shows the effect of additional PVP. The nanodispersed CNT concentration and intensities of individual subband peaks was increased by adding PVP to the solution. We noted

that even in the case of PVP, a sonication time of 40 min yielded the optimum condition for CNT concentration, consistent with Figure 2a. We can clearly see that the absorbance with PVP was enhanced by a factor of 3 compared to absorbance without PVP (Figure 3c). Here the absorbance and remaining CNT concentration was calculated from the absorption spectra at 902 nm similar to Figure 2c. The remaining CNT concentration was also almost doubled with PVP addition. This increase of the CNT concentration in the solution demonstrates the better utility of PVP as a dispersant. The slight difference in the factor was ascribed to the different extinction coefficient from the additional PVP in the solution.

To investigate the dispersion state of the samples more elaborately, Absorption spectroscopy, Raman spectroscopy, and fluorescence spectroscopy were used. Absorbances within a range of centrifugation speeds from 15 000g to 376 300g show subband peaks in Figure 4a, which is a characteristic of nanodispersion to some degree. The dotted lines indicate the positions of subbands of S11 region. At the low centrifugation speed region up to 112 800g, the subband peaks near 1165 and 994 nm were broad. We define this as region I, which is a mixture of nanodispersion (due to the appearance of subband peaks) and macrodispersion (due to the presence of yet-broad peaks at the S11 band). When the centrifugation speed exceeded 170 000g, as highlighted by the color, the peak near 1165 nm was clearly split into two peaks, and the peak near 994 nm was split into four peaks (see dotted line from 1 to 6). This region

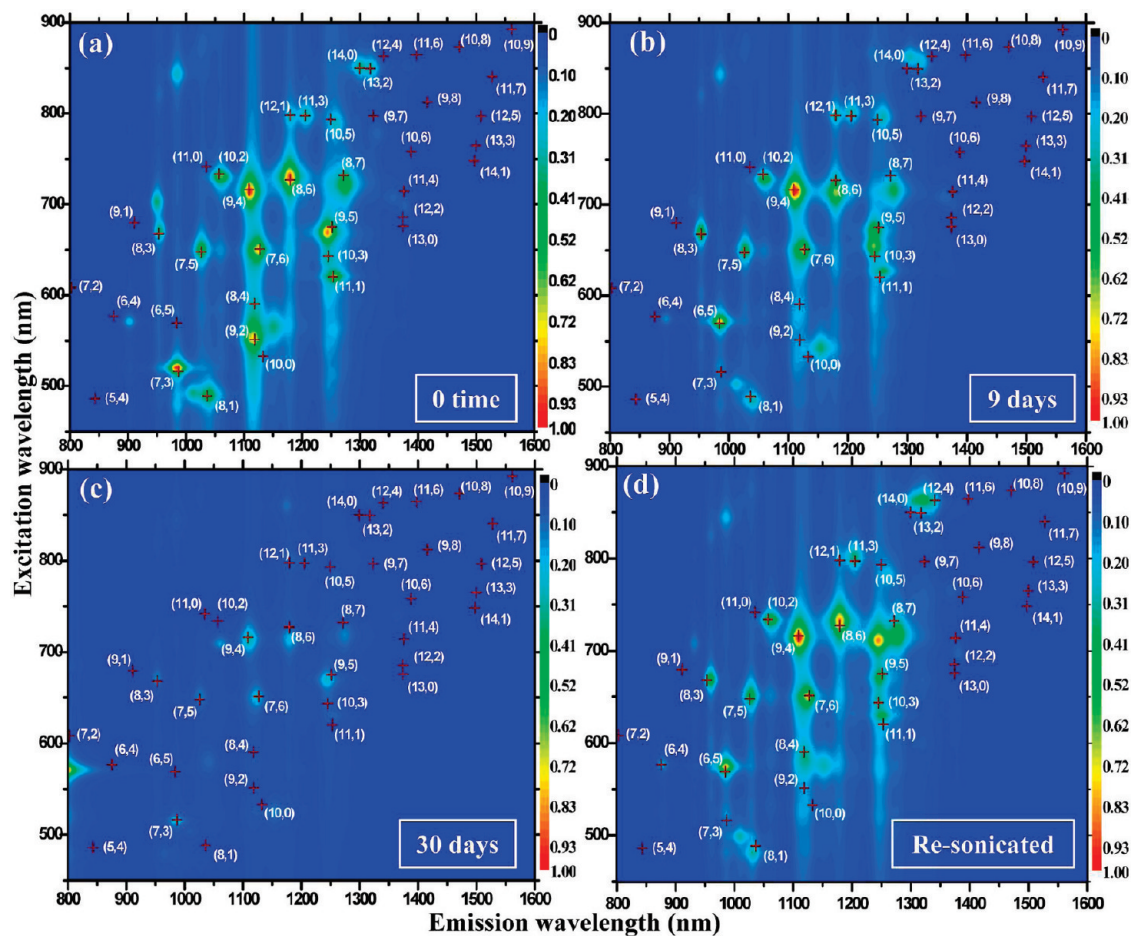


Figure 7. Contour plot of fluorescence intensity for excitation vs emission wavelengths similar to Figure 6c when the sample is left under ambient conditions (a) just after centrifugation, (b) after 9 days, (c) after 30 days, and (d) after re-sonication for 3 min following the previous 30 days.

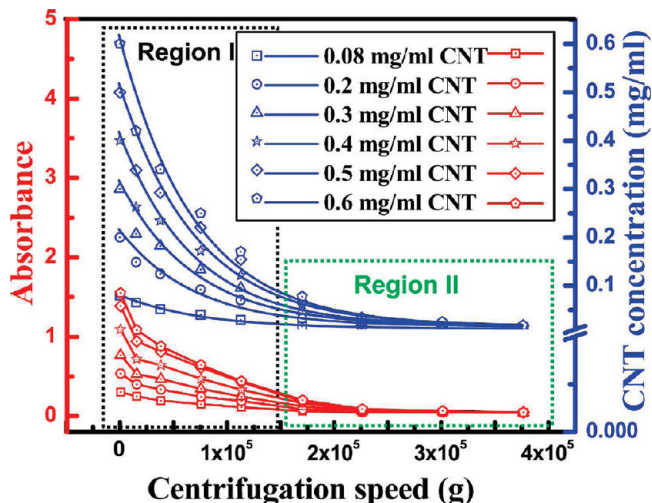


Figure 8. Centrifugation speed-dependent absorbance and final SWCNT concentration for a given initial CNT concentration of the SWCNTs solution (3 wt % SDS, 1 wt % PVP, 50 mL water, 40 min sonication at 9.38 W/mL power density and 9 °C constant temperature) has been plotted. All of the Y-axis values were obtained at the wavelength of 902 nm.

is defined as nanodispersion, region II. A similar distinction was also identified in Raman spectroscopy. In Figure 4b, the radial breathing mode (RBM) of the Raman spectra was obtained from SWCNT solution at a laser excitation energy of 1.96 eV at different centrifugation speeds. Two peaks near 194 and 217 cm⁻¹ in the powder sample disappeared in the dispersed

sample; furthermore, the others peaks were slightly upshifted.³⁰ It is well-known that debundling shifts the RBM slightly, such that the resonance condition could be violated.²⁹ This is a simple indication that the SWCNTs were well dispersed. Our main concern is the change of the peak near 252 (line 1) and 257 cm⁻¹ (line 2). The peak near 257 cm⁻¹ was broadly split in the dispersed CNT solution without centrifugation. With increasing centrifugation speed, this peak split into two peaks near 252 and 257 cm⁻¹. At 170 000g, the first peak near 252 cm⁻¹ abruptly became dominant compared to the second peak near 257 cm⁻¹ and simultaneously, the peak intensity near 283 cm⁻¹ increased abruptly as well. One intriguing phenomenon is the appearance of new peaks near 263 (line 3) and 299 cm⁻¹ (line 4). This state of dispersion persisted up to high centrifugation speed near 376 000g. The distinction of these two regions in the centrifugation speed is consistent with the results of absorption spectroscopy. It is generally believed that the nanodispersion of only semiconducting CNTs is identified by the peak splitting in the fluorescence spectra. The peak splitting in the RBMs of Raman spectra and absorption spectroscopy indicate that both methods could be another way of monitoring the dispersion state. Figure 4c represents the D-band peak area variation of Raman spectra with sonication time for the same samples used in Figure 2. It is clear from the graph that as the sonication time increased, the D-band peak area also increased, indicating an increase in number of defects on the CNTs. CNTs will be cut eventually and the length gets shorter. This decreases van der Waals interaction strength between CNTs and thus dispersion should be improved. The use of additional PVP

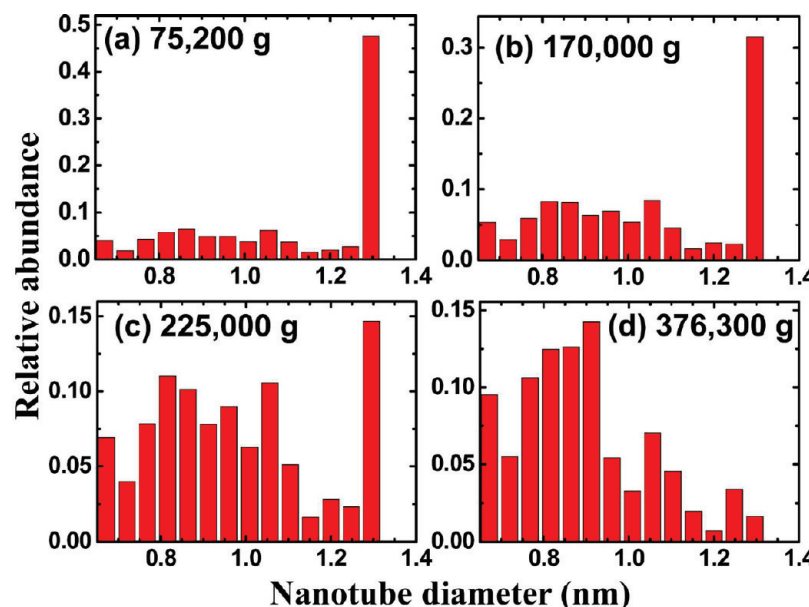


Figure 9. Diameter distribution of nanodispersed SWCNTs (initial CNT concentration 0.06 wt %, and all other parameters are same as Figure 8) at different centrifugation speeds obtained from fluorescence spectra.

generated relatively less number of defects. This indicates that sonication time should be used with care to minimize the number of defects to within a reasonable level. It is noted that our results with PVP show better dispersion than the previous works with other types of polymers.^{36,37}

Further investigation of the CNT dispersion state has been performed by SPM at DFM mode. Figure 5 represents the SPM images of the spin-coated CNT solution on silicon substrate. To increase adhesion between CNTs and silicon substrate, the substrate was functionalized by amine group from 1% amino-propyltriethoxy silane solution in anhydrous toluene. After spin coating of the CNT solution onto the functionalized Si substrate, various treatments were performed to remove the SDS as explained in the Figure caption. The deposited CNT solutions of Figure 5, panels a and b, belong to the respective region I which contains a mixed state of macro and nano dispersed SWCNTs and the region II which contains only nanodispersed SWCNTs. The dispersion state of the deposited SWCNTs has been clearly distinguished by these SPM images. Figure 5a contains both individually dispersed SWCNTs and small SWCNT bundles. The line profile from the image also proves wide distribution of nanotube diameters. It is noted that the diameters of SWCNTs looks swollen due to the presence of SDS on the CNT surface. Although the various treatments have been performed to remove the SDS contents in the sample, some SDS still remain in the substrate (aggregated due to heat treatment) and CNT walls. For this reason the diameter (from line profile) of the SWCNT has been observed higher than the fluorescence data. Figure 5(b) contains individual SWCNT only producing similar range of line profile heights, although few have higher height due to higher SDS residue in the CNT walls. By these SPM images, two dispersion states of the SWCNT dispersion are clearly confirmed, in good agreement with the prediction from Raman and absorption spectra.

3.2. Characterizations and Properties of Dispersed CNTs.

Figure 6, panels a and b, represents the measured fluorescence spectrum of nanodispersed CNT solution excited by laser energies of 1.94 (640 nm) and 1.58 eV (785 nm), respectively. Another fluorescence spectrum was obtained using laser excitation energy of 1.81 eV (683 nm) (not shown in the figure). These three measured spectra were individually fitted with Lorentzian

base functions for all possible transitions from 800 to 1600 nm. The measured and simulated curves showed excellent agreement, as shown in Figure 6, panels a and b. All of the chiral species were specified and intensities were marked by colors in Figure 6c. Numerous peaks were distinguishable, which is an indication of nanodispersion. Figure 6d is another way of representing an abundance of semiconducting SWCNTs with various chiral indices in the sample.

One intriguing phenomenon is the stability of the nanodispersed SWCNT solution, which has rarely been challenged.³⁴ We demonstrate that the stability of the solution can be monitored by the fluorescence plot, as shown in Figure 7. After 9 days, the intensities of most of the spots had diminished (Figure 7b). This indicates an aggregation of SWCNTs into bundles. After 30 days, almost all of the peaks had faded away except the high intensity peaks (Figure 7c). However, all of the peaks reappeared (Figure 7d), similar to the original sample in Figure 7a after resonication for 3 min. Even though the SWCNTs were aggregated after few days, their aggregation was loosely bound due to the presence of SDS on the surface of SWCNTs such that they became nanodispersed again by a simple sonication of 3 min. The similar phenomenon is expected from SWCNTs dispersed in SDS and PVP surfactant.

Another ambiguity in the CNT dispersion was the dependence of initial CNT concentration on the saturated nanodispersed CNT concentration at the final stage. Figure 8 shows absorbance (obtained from absorption spectra at 902 nm) as a function of centrifugation speed for a given initial SWCNT concentration. The CNT concentration was calculated using the absorbance relationship, $A = \epsilon \rho L$, or $\rho = (A/A_0)\rho_0$, where the initial and final absorbances A_0 and A are expressed in terms of extinction coefficient ϵ , the initial and final concentrations of SWCNTs ρ_0 and ρ , and the light path length L . In measuring initial CNT concentration, we ensured that no precipitated CNTs in the solution were found before centrifugation such that the nominal input CNT concentration was directly used for the initial CNT concentration. Independent of the initial SWCNT concentration, the remaining SWCNT concentration at the nanodispersion region of high centrifugation speed of 376 300g is almost constant. At the intermediate nanodispersion region near 170 000g, the final SWCNT concentration was proportional to

the initial SWCNT concentration. These curves were fitted using the relationship $C = C_0 \exp(-v/v_c)$, where C_0 is the initial CNT concentration, and v and v_c are the centrifugation speed and critical centrifugation speed, respectively. All of these curves were well-fitted with critical centrifugation speed $v_c = (0.7 \pm 0.0146) \times 10^5$ g. The nanodispersion was reached at about $2v_c$.

Once the emission energy and its intensity were obtained from the fluorescence spectra, information about the diameter distribution could be obtained from the modified Kataura plot.³¹ The most abundant SWCNT diameter after a centrifugation speed of 75 200g was 1.3 nm, although some portion of small diameter SWCNTs was distributed over a wide range of diameters. This distribution of diameters was persistent up to 225 800g, except small diameter distribution was increased gradually. Figure 9a–d shows the diameter distribution of the nanodispersed CNT solution at 75 200g, 170 000g, 225 800g, and 376 300g centrifugation speed for 4 h respectively. It was observed from the figure that the average diameters of the nanodispersed CNT (remains after centrifugation) become shorter as the centrifugation speed increases. The explanation could be due to the fact that larger diameter tubes have more atoms and more surface area compared to the small diameter CNTs, which induces more SDS and PVP adsorption to large diameter SWCNT surface, creating more pull on the large diameter nanotubes during high centrifugation, and precipitates at the bottom of the solution. To our knowledge, this is the first report that diameters can be sorted out by centrifugation.

4. Conclusion

We have demonstrated optimization procedures to obtain nanodispersion and a mixed state of nanodispersion with macro-dispersion states of HiPCO SWCNTs in water by optimizing the amount of surfactants, sonication time, and centrifugation conditions. 3 wt % of SDS surfactant, 40 min sonication (9.38 W/mL sonication power density), and centrifugation speed higher than 170 000g (above $2v_c$) were favorable to produce individually nanodispersed SWCNT solution. Raman spectroscopy, optical absorption spectroscopy, and fluorescent spectroscopy consistently demonstrated two phases of dispersion states ((i) a mixed state of macro-dispersion and nanodispersion, and (ii) nanodispersion) which was controlled by the centrifugation speed. The saturated SWCNT concentration was nearly constant at high centrifugation speed independent of the initial SWCNT concentration. We also demonstrated the stability and recovery of the nanodispersion using fluorescent spectroscopy. Furthermore, we were also able to sort out diameters of SWCNTs by controlling centrifugation speed. Our systematic approach for controlling nanodispersion with high SWCNT concentration and diameter selectivity can be adopted in many different applications in the future.

Acknowledgment. This work was supported by the MOEST through the Star-Faculty project, a grant from the TND Programs, in part KOSEF through the CNNC at SKKU, WCU program through the KOSEF funded by the MOEST (R31-2008-000-10029-0), by grants from AFOSR, the KRF Grant funded by the Korean Government (MOEST) (KRF-2008-211-D00011), and support by National Science Foundation EEC-0738320.

References and Notes

- (1) Monthoux, M.; Kuznetsov, V. L. *Carbon* **2006**, *44*, 1621.
- (2) Iijima, S. *Nature (London)* **1991**, *354*, 56.
- (3) Thess, A.; Lee, R.; Nikolaev, P.; Dai, H.; Petit, P.; Robert, J.; Xu, C.; Lee, Y. H.; Kim, S. G.; Colbert, D. T.; Scuseria, G.; Tomanek, D.; Fischer, J. E.; Smalley, R. E. *Science* **1996**, *273*, 483.
- (4) An, K. H.; Lee, Y. H. *Nano* **2006**, *1*, 115.
- (5) Zhou, C.; Kong, J.; Yenilmez, E.; Dai, H. *Science* **2000**, *290*, 1552.
- (6) Coleman, J. N.; Khan, U.; Gun'ko, Y. K. *Adv. Mater.* **2006**, *18*, 689.
- (7) Ajayan, P. M.; Schadler, L. S.; Giannaris, C.; Rubio, A. *Adv. Mater.* **2000**, *12*, 750.
- (8) Hwang, E. S.; Cao, C.; Hong, S.; Jung, H. J.; Cha, C. Y.; Choi, J. B.; Kim, Y. J.; Baik, S. *Nanotechnology* **2006**, *17*, 3442.
- (9) Hata, K.; Futaba, D. N.; Mizuno, K.; Namai, T.; Yumura, M.; Iijima, S. *Science* **2004**, *306*, 1362.
- (10) Tans, S. J.; Verschueren, A. R. M.; Dekker, C. *Science* **1998**, *393*, 49.
- (11) Rueckes, T.; Kim, K.; Joelevich, E.; Tseng, G. Y.; Cheung, C. L.; Lieber, C. M. *Science* **2000**, *289*, 94.
- (12) (a) Collins, P. G.; Arnold, M. S.; Avouris, P. *Science* **2001**, *292*, 706. (b) Sun, C. H.; Yin, L. C.; Lu, F.; Li, G. Q.; Cheng, H. M. *Chem. Phys. Lett.* **2005**, *403*, 343. (c) Moon, J. M.; Park, Y. S.; An, K. H.; Park, G. S.; Lee, Y. H. *J. Phys. Chem. B* **2001**, *105*, 5677.
- (13) Kim, K. K.; Yoon, S. M.; Choi, J. Y.; Lee, J.; Kim, B. K.; Kim, J. M.; Lee, J. H.; Paik, U.; Park, M. H.; Yang, C. W.; An, K. H.; Chung, Y.; Lee, Y. H. *Adv. Funct. Mater.* **2007**, *17*, 1775.
- (14) Zhao, W.; Song, C.; Pehrsson, P. E. *J. Am. Chem. Soc.* **2002**, *124*, 12418.
- (15) (a) An, K. H.; Park, K. A.; Heo, J. G.; Lee, J. Y.; Jeon, K. K.; Lim, S. C.; Yang, C. M.; Lee, Y. S.; Lee, Y. H. *J. Am. Chem. Soc.* **2003**, *125*, 3057. (b) Michelson, E. T.; Chiang, I. W.; Zimmerman, J. L.; Boul, P. J.; Lozano, J.; Li, J.; Smalley, R. E.; Hauge, R. H.; Margrave, J. L. *J. Phys. Chem. B* **1999**, *103*, 4318.
- (16) Kim, K. K.; Bae, D. J.; Lee, J. Y.; An, K. Y.; Yang, C. M.; Lee, Y. H. *J. Nanosci. Nanotechnol.* **2005**, *5*, 1055.
- (17) Furtado, C. A.; Kim, U. J.; Gutierrez, H. R.; Pan, L.; Dickey, E. C.; Eklund, P. C. *J. Am. Chem. Soc.* **2004**, *126*, 6095.
- (18) Richard, C.; Balavoine, F.; Schulta, P.; Ebbesen, T. W.; Mioskowski, C. *Science* **2003**, *300*, 775.
- (19) Matarredona, O.; Rhoads, H.; Li, Z.; Harwell, J. H.; Blazano, L.; Resasco, D. E. *J. Phys. Chem. B* **2003**, *107*, 13357.
- (20) Moore, V. C.; Strano, M. S.; Haroz, E. H.; Hauge, R. H.; Smalley, R. E. *Nano Lett.* **2003**, *3*, 1379.
- (21) O'Connell, M. J.; Boul, P.; Ericson, L. M.; Huffman, C.; Wang, Y.; Haroz, E.; Kuper, C.; Tour, J.; Ausman, K. D.; Smalley, R. E. *Chem. Phys. Lett.* **2001**, *342*, 265.
- (22) Zheng, M.; Jagota, A.; Semke, E. D.; Diner, B. A.; McLean, R. S.; Lustig, S. R.; Richardson, R. E.; Tassi, N. G. *Nature (London)* **2003**, *2*, 338.
- (23) O'Connell, M. J.; Boul, P.; Ericson, L.; Huffman, C.; Wang, Y.; Haroz, E.; Kuper, C.; Tour, J.; Ausman, K. D.; Smalley, R. E. *Chem. Phys. Lett.* **2001**, *342*, 265.
- (24) Star, A.; Steuerman, D. W.; Heath, J. R.; Stoddart, J. F. *Angew. Chem., Int. Ed.* **2002**, *41*, 2508.
- (25) Napper, D. H. *Polymeric Stabilization of Colloidal Dispersion*; Academic Press: London, 1983.
- (26) Geng, H. Z.; Lee, D. S.; Kim, K. K.; Han, G. H.; Park, H. K.; Lee, Y. H. *Chem. Phys. Lett.* **2008**, *455*, 275.
- (27) Moore, V. C.; Strano, M. S.; Haroz, E. H.; Hauge, R. H.; Smalley, R. E. *Nano Lett.* **2003**, *3* (10), 1379.
- (28) Utsumi, S.; Kanamaru, M.; Honda, H.; Kanoh, H.; Tanaka, H.; Ohkubo, T.; Sakai, H.; Abe, M.; Kaneko, K. *J. Colloid Interface Sci.* **2007**, *308*, 276.
- (29) Rao, A. M.; Chen, J.; Richter, E.; Schlecht, U.; Eklund, P. C.; Haddon, R. C.; Venkateswaran, U. D.; Kwon, Y. K.; Tománek, D. *Phys. Rev. Lett.* **2001**, *86* (17), 3895(4).
- (30) Weisman, R. B.; Bachilo, S. M. *Nano Lett.* **2003**, *3* (9), 1235.
- (31) Bachilo, S. M.; Strano, M. S.; Kittrell, C.; Hauge, R. H.; Smalley, R. E.; Weisman, R. B. *Science* **2002**, *298*, 2361.
- (32) O'Connell, M. J.; Bachilo, S. M.; Huffman, C. B.; Moore, V. C.; Strano, M. S.; Haroz, E. H.; Rialon, K. L.; Boul, P. J.; Noon, W. H.; Kittrell, C.; Ma, J.; Hauge, R. H.; Weisman, R. B.; Smalley, R. E. *Science* **2002**, *297*, 593.
- (33) Islam, M. F.; Rojas, E.; Bergey, D. M.; Johnson, A. T.; Yodh, A. G. *Nano Lett.* **2003**, *3* (2), 269.
- (34) Wang, H.; Zhou, W.; Ho, D. L.; Winey, K. I.; Fischer, J. E.; Glinka, C.; Hobbie, E. K. *Nano Lett.* **2004**, *4* (1), 789.
- (35) Fagan, J. A.; Landi, B. J.; Mandelbaum, I.; Simpson, J. R.; Bajpai, V.; Bauer, B. J.; Migler, K. A.; Walker, R. H.; Raffaelle, R.; Hobbie, E. K. *J. Phys. Chem. B* **2006**, *110*, 23801.
- (36) Chen, F.; Wang, B.; Chen, Y.; Li, L. J. *Nano Lett.* **2007**, *7*, 10–3013.
- (37) Nish, A.; Hwang, J. Y.; Doig, J.; Nicholas, R. J. *Nat. Nanotechnol.* **2007**, *2*, 640.
- (38) Geng, H. Z.; Kim, K. K.; Lee, K.; Kim, G. Y.; Choi, H. K.; Lee, D. S.; Hyeok, H. K.; Lee, Y. H. *Nano* **2007**, *2*, 3–157.